Pentaquark Θ^+ production via $\gamma N \to \bar{K}^* \Theta^+(3/2^\pm)$

Seung-Il Nam,[1,*] Atsushi Hosaka,[2,†] and Hyun-Chul Kim[1,‡]
[1]*Department of Physics and Nuclear Physics & Radiation Technology Institute (NuRI), Pusan National University, Busan 609-735, Korea*
[2]*Research Center for Nuclear Physics (RCNP), Ibaraki, Osaka 567-0047, Japan*
(Received 31 October 2005; published 18 August 2006)

We study the photoproduction of the exotic pentaquark Θ^+ baryon with the vector kaon, assuming that the quantum numbers of the Θ^+ to be $J^P = 3/2^\pm$ and $J^P = 1/2^+$. Scalar meson $\kappa(800)$ exchange is also taken into account. In contrast with the $\gamma N \to \bar{K}\Theta^+(3/2^\pm)$ process, the large suppression from the proton target is not observed in the total cross sections. We also suggest a method to determine which meson exchange is the most dominant by analyzing the polarizations of incident photon and outgoing K^*. We find that κ exchange turns out to be prominent when the polarizations of the photon and K^* are aligned to be parallel, whereas K exchange predominates when they are perpendicular to each other.

DOI: 10.1103/PhysRevC.74.025204 PACS number(s): 13.75.Cs, 14.20.−c

I. INTRODUCTION

Since Diakonov *et al*. predicted the mass and width of the pentaquark baryon Θ^+ [1], there has been a great deal of works to clarify its existence and properties. Although various experiments have reported the existence of Θ^+ after the first observation by the LEPS collaboration [2], the situation is not yet settled down primarily due to the relatively low statistics of the low-energy experiments. Furthermore, in almost all high-energy experiments, the Θ^+ has not been seen (see, for example, a recent review [3–5] for the compilation of the experimental results).

Recently, the CLAS collaboration has reported null results for finding the Θ^+ in the reactions $\gamma p \to \bar{K}^0 K^+ n$ [6], $\gamma d \to \bar{p} K^- K^+ n$ [7], and $\gamma d \to \bar{\Lambda} n K^+$ [8]. The upper limits of the cross sections of producing Θ^+ were estimetaed to be, for instance, $\sigma(\gamma p \to \bar{K}^0 \Theta^+) \sim 0.8$ nb, $\sigma(\gamma n \to \bar{K}^- \Theta^+) \sim 3$ nb. Though these experiments had high statistics, their results do not yet lead to the absence of Θ^+ immediately, because the updatd positive evidences also seem rather convincing. In the LEPS, they observe a peak for the Θ^+ in the reaction $\gamma d \to \bar{\Lambda}(1520) n K^+$ [9] when the $\Lambda(1520)$ is detected in the forward angle region. DIANA reported further evidence in the reaction $K^+ n \to K^0 p$ on a neutron bound in the Xenon nucleus [10]. The statistical significance of the DIANA measurement is $4.3 \sim 7.3\,\sigma$. Moreover, KEK-PS E522 experiment has reported a measurement of the Θ^+ via the reaction $\pi^- p \to K^- X$ [11], although the statistical siginificance is not large enough.

Experimentally, the two similar experiments from CLAS and LEPS are not in contradiction, because they measure different regions; CLAS detects final particles in the region where the scattering angle is not small, whereas the LEPS observes the forward angle region, and their measuring regions have little overlap.

Theoretically, it was suggested that the production rate of the Θ^+ from the proton target is considerably suppressed as compared to the case of the neutron target, if the spin of Θ^+ is 3/2 [12]. Furthermore, in this case, the cross section of the neutron target that is larger than the proton case is strongly forward peaking. These may explain the different observations of the CLAS and LEPS. Interestingly, a similar suppression is found in the $\Lambda(1520)$ photoproduction [13], though in this case the suppression takes place for the neutron target. Therefore, it should be fair to say that the existance of the Θ^+ is not yet excluded.

Motivated by the previous work [13], we continue to investigate the Θ^+ photoproduction with the vector kaon K^*, based on the effective Lagrangian approach with phenomenological form factors. Here, we consider the cases with $J^P = 3/2^\pm$ and $J^P = 1/2^+$ for the Θ^+ baryon. Scalar meson $\kappa(800, 0^+)$ exchange is also taken into account, in addition to pseudoscalar K and vector K^* exchanges. We note that κ exchange in the t channel does not appear in the $\gamma N \to \bar{K}\Theta^+$ reaction process because the $\gamma\kappa K$ coupling is not allowed [12], whereas κ exchange is possible in the present reaction process according to the existence of the $\gamma\kappa K^*$ coupling. The role of κ may be interesting if it is dominated by a tetraquark component that has been suggested to have a strong coupling to exotic baryons [14].

One of the interesting features of the present reaction process is that there are two polarizations in the initial and final states: the polarizations of the incident photon and the outgoing K^*. By making a proper combination of these two polarizations, one can determine which meson exchange in the t channel dominates the reaction process.

The outline of the present work is as follows: In Sec. II, we define the effective Lagrangians for the $\gamma N \to \bar{K}^* \Theta^+(3/2^\pm)$ reaction and calculate the invariant amplitudes with phenomenological form factors. The numerical results are given and discussed for the $\Theta^+(3/2^\pm)$ and $\Theta^+(1/2^+)$ in Sec. III. Section IV is devoted to a reaction analysis via the photon and K^* polarizations. We summarize our results and draw conclusions in the final section.

*Electronic address: sinam@pusan.ac.kr
†Electronic address: hosaka@rcnp.osaka-u.ac.jp
‡Electronic address: hchkim@pusan.ac.kr

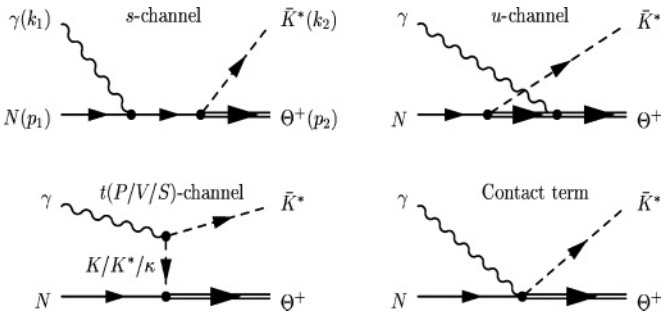

FIG. 1. Born diagrams calculated in the effective Lagrangian approach. $P/V/S$ in the t channel stand for the pseudoscalar kaon, vector kaon, and scalar κ exchanges, respectively.

II. FORMALISM

We investigate the reaction $\gamma N \to \bar{K}^* \Theta^+$ at the tree level, i.e., in the Born approximation. The relevant Feynman diagrams are drawn in Fig. 1, where we define the four-momenta of the particles involved in the process. For convenience, we denote the spin $3/2$ and $1/2$ Θ^+ with the subscripts 3 and 1, respectively.

The effective Lagrangians pertinent to the present work are given as follows: First, we consider the vertices of photon-meson-meson couplings:

$$\mathcal{L}_{\gamma K K^*} = g_{\gamma K K^*} \epsilon_{\mu\nu\sigma\rho} (\partial^\mu A^\nu)(\partial^\sigma K) K^{*\rho} + \text{h.c.}, \quad (1)$$

$$\mathcal{L}_{\gamma K^* K^*} = ie[K^{*\dagger}_\nu (\partial_\mu K^{*\nu}) - K^*_\nu (\partial_\mu K^{*\dagger\nu})] A^\mu, \quad (2)$$

where K, K^*, and A^μ denote the pseudoscalar kaon, vector kaon, and photon fields, respectively. We employ the effective Lagrangian taken from Refs. [15–18]. Note that to maintain gauge invariance of the reaction amplitudes, we introduce a vector-meson exchange model using the $\gamma K^* K^*$ vertex as shown in Eq. (2), which was suggested by Refs. [19,20]. This vertex represents three vector particle coupling that manifests the nature of the non-Abelian gauge fields.

The baryon electromagnetic couplings for the nucleon and the spin $3/2$ and $1/2$ Θ^+ are defined as follows:

$$\mathcal{L}_{\gamma NN} = -e\bar{N}\left[\not{A} + \frac{\kappa_N}{4M_N}\sigma_{\mu\nu}F^{\mu\nu}\right] N + \text{h.c.}, \quad (3)$$

$$\mathcal{L}_{\gamma \Theta_1 \Theta_1} = -e\bar{\Theta}_1\left[\not{A} + \frac{\kappa_\Theta}{4M_\Theta}\sigma_{\mu\nu}F^{\mu\nu}\right] \Theta_1 + \text{h.c.}, \quad (4)$$

$$\mathcal{L}_{\gamma \Theta_3 \Theta_3} = -e\bar{\Theta}^\mu_3 g_{\mu\nu}\left[\not{A} + \frac{\kappa_\Theta}{4M_\Theta}\sigma_{\sigma\rho}F^{\sigma\rho}\right] \Theta^\nu_3 + \text{h.c.}, \quad (5)$$

where N, Θ^μ_3, and Θ_1 stand for the nucleon, the spin $3/2$ Rarita-Schwinger (RS) Θ^+ [21] and spin $1/2$ Θ^+, respectively. The same structures of the Lagrangians are used for the nucleon and spin $1/2$ Θ^+ [Eqs. (3) and (4)]. Following Ref. [22], we construct the effective Lagrangian for the electromagnetic coupling of the spin $3/2$ Θ^+ in Eq. (5). Here, being different from Ref. [22], because the electric quadrapole ($E2$) and magnetic octupole ($M3$) form factors are expected to be small, compared to the charge and magnetic dipole form factors of spin $3/2$ baryons, we consider only the $E0$ and $M1$ electromagnetic interactions. Concerning other possible structures of the electromagnetic couplings, it is worth mentioning that, as indicated in Ref. [21], the electromagnetic coupling for the spin $3/2$ Θ^+ can be reconstructed equivalently with the terms such as $\bar{\Theta}^\mu F_{\mu\nu}\Theta^\nu$ and others.

The $K(K^*)N\Theta$ vertices for the spin $3/2$ and $1/2$ Θ^+ baryons are defined as follows [13,23]:

$$\mathcal{L}_{KN\Theta_3} = \frac{g_{KN\Theta_3}}{M_K}\bar{\Theta}^\mu_3 \partial_\mu K \Gamma_5 N + \text{h.c.}, \quad (6)$$

$$\mathcal{L}_{KN\Theta_1} = i g_{KN\Theta_1}\bar{\Theta}_1 \Gamma_5 \gamma_5 K N + \text{h.c.}, \quad (7)$$

$$\mathcal{L}_{K^*N\Theta_3} = -\frac{i g_{K^*N\Theta_3}}{M_{K^*}}\bar{\Theta}_{3,\mu}\gamma_\nu F^{\mu\nu}_{K^*}\Gamma_5\gamma_5 N + \text{h.c.}, \quad (8)$$

$$\mathcal{L}_{K^*N\Theta_1} = g^V_{K^*N\Theta_1}\bar{\Theta}_1\gamma_\mu\Gamma_5 K^{*\mu} N - \frac{g^T_{K^*N\Theta_1}}{2(M_\Theta + M_N)} \times \bar{\Theta}_1\Gamma_5\sigma_{\mu\nu}F^{\mu\nu}_{K^*} N + \text{h.c.}, \quad (9)$$

where Γ_5 denotes $\mathbf{1}_{4\times4}$ in the positive-parity and γ_5 for the negative-parity Θ^+, respectively, for both cases of the spin $3/2$ and spin $1/2$. $F^{\mu\nu}_{K^*}$ stands for $\partial^\mu K^{*\nu} - \partial^\nu K^{*\mu}$. As for the spin $1/2$ Θ^+, we consider only the pseudoscalar coupling scheme for the $KN\Theta$ vertex due to the approximate equivalence between the pseudoscalar and psedovector schemes [24]. On the contrary, only pseudovector (derivative) coupling is possible for the case of the spin $3/2$ due to the constraint $\gamma_\mu\Theta^\mu = 0$. Concerning the $K^*N\Theta$ vertex of Eqs. (8) and (9), we consider the Lagrangian structures that are necessary minimally for maintaining the gauge invariance when we construct reaction amplitudes. Note that, as for the spin $1/2$ case, we have the vector and tensor terms in the Lagrangian of Eq. (9). Here, we use the value of $g^T_{K^*N\Theta_1} = |g^V_{K^*N\Theta_1}|$ as a trial because no experimental data are available now. However, the strength of $g^T_{K^*N\Theta}$ can be estimated from the recent calculations of the transition magnetic moment of $\gamma N_8 N^*_{\bar{1}0}$, where $\kappa_{\gamma N_8 N^*_{\bar{1}0}}$ was found to be $0 \sim 0.5$ [25–27]. Here, $N^*_{\bar{1}0}$ is a nucleon partner of the antidecuplet pentaquark. Assuming the vector dominance and flavor SU(3) symmetry, we expect that the ratio $|g^T_{K^*N\Theta}/g^V_{K^*N\Theta}|$ is less than unity. Thus, our choice of $g^T_{K^*N\Theta_1} = |g^V_{K^*N\Theta_1}|$ can be almost its upper bound.

Finally, we introduce the photon coupling in the $K^*N\Theta$ vertex by minimal substitution, $\partial_\mu \to \partial_\mu + i\hat{Q}A_\mu$ where $\hat{Q}$ is the charge matrix acting on the matter fields.

$$\mathcal{L}_{\gamma K^* N\Theta_3} = \frac{e g_{K^*N\Theta_3}}{M_{K^*}}\bar{\Theta}^\mu_3\gamma^\nu[A_\mu K^*_\nu - A_\nu K^*_\mu]\Gamma_5\gamma_5 N + \text{h.c.}, \quad (10)$$

$$\mathcal{L}_{\gamma K^* N\Theta_1} = -\frac{i e g^T_{K^*N\Theta_1}}{2(M_\Theta + M_N)} \times \bar{\Theta}_1\Gamma_5\sigma_{\mu\nu}(A^\mu K^{*\nu} - A^\nu K^{*\mu}) N + \text{h.c.}. \quad (11)$$

These interaction vertices are related to the Feynman diagram of the contact term shown in Fig. 1. We note that the same interactions of Eqs. (10) and (11) are obtained from the non-Abelian terms of the covariant field tensor $\partial_\mu V_\nu - \partial_\nu V_\mu - i[V_\mu, V_\nu]$ with V_μ being an SU(3) vector meson field, and by using the vector dominance.

In Table I, we list the parameters (elecgromagnetic and strong couplings) that are used for numerical calculation. The nucleon magnetic moments κ_N and the $\gamma K^* K$ coupling constants are taken from experiments [28]. For $g_{KN\Theta}$, we

TABLE I. Parameters of the couplings used in the numerical calculations.

	κ_N		$g_{\gamma KK^*}$		$g_{KN\Theta_3}$	$g^V_{K^*N\Theta_3}$	$g_{KN\Theta_1}$	$g^V_{K^*N\Theta_1}$	$g^T_{K^*N\Theta_1}$
n	-1.91	Neutral	0.388/GeV	$\pi(\Theta) = +1$	0.53	$0.91 = 0.53\sqrt{3}$	1	$\sqrt{3}$	$\sqrt{3}$
p	1.79	Charged	0.254/GeV	$\pi(\Theta) = -1$	4.22	2.0	—	—	—

assume $\Gamma_{\Theta\to KN} = 1$ MeV and $M_\Theta = 1540$ MeV for both spins 3/2 and 1/2 [28]. For $g^V_{K^*N\Theta}$, we assume the estimation in the quark model $g^V_{K^*N\Theta} = \sqrt{3} g_{KN\Theta}$ for the positive-parity Θ^+ [29], whereas we used the results of Ref. [30] for $\Theta^+(3/2^-)$. As for the value of the anomalous magnetic moment of Θ^+, we set it to be unity for both spins as a trial. We show later that the dependence on κ_Θ is negligible, because the u-channel contributions turn out to be very small. Because we verified that the sign of $g^V_{K^*N\Theta}$ does not influence much on the results as shown in the previous work [12], we consider only the plus sign form. The case of $\Theta(1/2^-)$ is not studied because we verified that it behaves very similarly to that of $\Theta(1/2^+)$ except for the only obvious difference in the order of magnitudes being smaller by factor about 10 [24]. We note that in the present work, we do not consider nucleon resonance (N^*) contributions. In other words, we only take into account the minimally possible reaction diagrams as shown in Fig. 1.

Thus, the reaction amplitudes for spin 3/2 ($\mathcal{M}_3$) and 1/2 ($\mathcal{M}_1$) can be written as follows. Furthermore, we have checked that the amplitudes calculated from the Lagrangians satisfy the Ward-Takahashi identity with the form factors:

$$
\begin{aligned}
i\mathcal{M}_{3,s} &= -\frac{ieg_{K^*N\Theta}}{M_{K^*}}\bar{u}(p_2)[(k_2\cdot\epsilon_\Theta)\not\epsilon_{K^*} \\
&\quad -(\epsilon_\Theta\cdot\epsilon_{K^*})\not k_2]\Gamma_5\gamma_5\frac{(\not p_1 + M_N)F_c + \not k_1 F_s}{q_s^2 - M_N^2}\not k_1 u(p_1) \\
&\quad -\frac{ie\kappa_N g_{K^*N\Theta}}{2M_N M_{K^*}}\bar{u}(p_2)[(k_2\cdot\epsilon_\Theta)\not\epsilon_{K^*} - (\epsilon_\Theta\cdot\epsilon_{K^*})\not k_2] \\
&\quad \times\Gamma_5\gamma_5\frac{(\not q_s + M_N)F_s}{q_s^2 - M_2^2}\not\epsilon_\gamma\not k_1 u(p_1), \\
i\mathcal{M}_{3,u} &= -\frac{ieg_{K^*N\Theta}}{M_{K^*}}\bar{u}(p_2)\not\epsilon_\gamma\frac{(\not p_2 + M_\Theta)F_c + \not k_1 F_u}{q_u^2 - M_\Theta^2} \\
&\quad \times[(k_2\cdot\epsilon_\Theta)\not\epsilon_{K^*} - (\epsilon_\Theta\cdot\epsilon_{K^*})\not k_2]\Gamma_5\gamma_5 u(p_1) \\
&\quad -\frac{ie\kappa_\Theta g_{K^*N\Theta}}{2M_\Theta M_{K^*}}\bar{u}(p_2)\not\epsilon_\gamma\not k_1\frac{(\not q_u + M_\Theta)F_u}{q_u^2 - M_\Theta^2} \\
&\quad \times[(k_2\cdot\epsilon_\Theta)\not\epsilon_{K^*} - (\epsilon_\Theta\cdot\epsilon_{K^*})\not k_2]\Gamma_5\gamma_5 u(p_1), \\
i\mathcal{M}_{3,t(P)} &= -\frac{g_{\gamma KK^*}g_{KN\Theta}}{M_K}\frac{\bar{u}(p_2)\Gamma_5 u(p_1)}{q_t^2 - M_K^2} \\
&\quad \times\left[(\epsilon_\Theta\cdot q_t)\epsilon_{\mu\nu\sigma\rho}k_1^\mu\epsilon_\gamma^\nu q_t^\sigma\epsilon_{K^*}^\rho\right]F_t, \\
i\mathcal{M}_{3,t(V)} &= -\frac{ieg_{K^*N\Theta}}{M_{K^*}}\bar{u}(p_2)\frac{2\epsilon_\gamma\cdot k_2}{q_t^2 - M_{k^*}^2}[(q_t\cdot\epsilon_\Theta)\not\epsilon_{K^*} \\
&\quad -(\epsilon_\Theta\cdot\epsilon_{K^*})\not q_t]\Gamma_5\gamma_5 u(p_1)F_c, \\
i\mathcal{M}_{3,c} &= -\frac{ieg_{K^*N\Theta}}{M_{K^*}}\bar{u}(p_2)[(\epsilon_\gamma\cdot\epsilon_\Theta)\not\epsilon_{K^*} \\
&\quad -(\epsilon_\Theta\cdot\epsilon_{K^*})\not\epsilon_\gamma]\Gamma_5\gamma_5 u(p_1)F_c
\end{aligned}
\tag{12}
$$

and

$$
\begin{aligned}
i\mathcal{M}_{1,s} &= ieg^V_{K^*N\Theta_1}\bar{u}(p_2)\not\epsilon_{K^*}\Gamma_5\frac{(\not p_1 + M_N)F_c + \not k_1 F_c}{q_s^2 - M_N^2} \\
&\quad \times\not\epsilon_\gamma u(p_2) + \frac{ie\kappa_N g^V_{K^*N\Theta_1}}{2M_N}\bar{u}(p_2)\not\epsilon_{K^*}\Gamma_5 \\
&\quad \times\frac{(\not q_s + M_N)F_s}{q_s^2 - M_N^2}\not k_1\not\epsilon_\gamma u(p_2) + \frac{ieg^T_{K^*N\Theta_1}}{2(M_\Theta + M_N)} \\
&\quad \times\bar{u}(p_2)\Gamma_5(\not k_2\not\epsilon_{K^*} - \not\epsilon_{K^*}\not k_2)\frac{(\not p_1 + M_N)F_c + \not k_1 F_s}{q_s^2 - M_N^2} \\
&\quad \times\not\epsilon_\gamma u(p_2) - \frac{ie\kappa_N g^T_{K^*N\Theta_1}}{4M_N(M_\Theta + M_N)}\bar{u}(p_2)\Gamma_5(\not k_2\not\epsilon_{K^*} \\
&\quad -\not\epsilon_{K^*}\not k_2)\frac{\not p_1 + \not k_1 + M_N}{q_s^2 - M_N^2}\not\epsilon_\gamma\not k_1 u(p_2)F_s, \\
i\mathcal{M}_{1,u} &= ieg^V_{K^*N\Theta_1}\bar{u}(p_2)\not\epsilon_\gamma\frac{(\not p_s + M_\Theta)F_c - \not k_1 F_u}{q_u^2 - M_\Theta^2} \\
&\quad \times\not\epsilon_{K^*}\Gamma_5 u(p_1) + \frac{ie\kappa_\Theta g^T_{K^*N\Theta_1}}{4M_\Theta(M_\Theta + M_N)}\bar{u}(p_2)\not k_1\not\epsilon_\gamma \\
&\quad \times\frac{(\not q_u + M_\Theta)F_s}{q_u^2 - M_\Theta^2}\not\epsilon_{K^*}\Gamma_5 u(p_1) + \frac{ieg^T_{K^*N\Theta_1}}{2(M_\Theta + M_N)} \\
&\quad \times\bar{u}(p_2)\not\epsilon_\gamma\frac{(\not p_2 + M_\Theta)F_c - \not k_1 F_u}{q_u^2 - M_\Theta^2}\Gamma_5 \\
&\quad \times(\not k_2\not\epsilon_{K^*} - \not\epsilon_{K^*}\not k_2)u(p_2) - \frac{ie\kappa_\Theta g^T_{K^*N\Theta_1}}{4M_\Theta(M_\Theta + M_N)} \\
&\quad \times\bar{u}(p_2)\not k_1\not\epsilon_\gamma\frac{\not p_2 - \not k_1 + M_\Theta}{q_u^2 - M_\Theta^2}\Gamma_5 \\
&\quad \times(\not k_2\not\epsilon_{K^*} - \not\epsilon_{K^*}\not k_2)u(p_2)F_u, \\
i\mathcal{M}_{1,t(P)} &= g_{KN\Theta_1}g_{\gamma KK^*}\frac{\bar{u}(p_1)\Gamma_5\gamma_5 u(p_1)}{q_t^2 - M_K^2}\epsilon_{\mu\nu\rho\sigma}k_1^\mu\epsilon_\gamma^\nu\epsilon_{K^*}^\rho q_t^\sigma F_t, \\
i\mathcal{M}_{1,t(V)} &= -2ieg_{K^*N\Theta_1}\bar{u}(p_1)\frac{k_2\cdot\epsilon_\gamma\not\epsilon_{K^*}\Gamma_5}{q_t^2 - M_{K^*}^2}u(p_1)F_c \\
&\quad +\frac{ie\kappa_N g^T_{K^*N\Theta_1}}{M_\Theta + M_N}\bar{u}(p_2)\Gamma_5(\not q_t\not\epsilon_{K^*} - \not\epsilon_{K^*}\not q_t) \\
&\quad \times\frac{k_2\cdot\epsilon_\gamma}{q_t^2 - M_{K^*}^2}u(p_1)F_c, \\
i\mathcal{M}_{1,c} &= \frac{ieg^T_{K^*N\Theta_1}}{2(M_\Theta + M_N)}\bar{u}(p_2)\Gamma_5(\not\epsilon_\gamma\not\epsilon_{K^*} - \not\epsilon_{K^*}\not\epsilon_\gamma)u(p_1)F_c.
\end{aligned}
\tag{13}
$$

The subscripts $s, u, t(P), t(V)$, and c of $\mathcal{M}$ indicate s, u, pseudoscalar K exchange, vector K^* exchange, and the contact term, respectively. $q_s = p_1 + k_1$, $q_t = k_1 - k_2$, and $q_u = p_1 - k_2$ are the momentum transfers for each kinematical channel.

The Mandelstam variables s, t, and u are defined in a standard way: $s = q_s^2$, $u = q_u^2$, and $t = q_t^2$. For spin $3/2$ Θ^+, we need to take into account $\mathcal{M}_{s,E,M}$, $\mathcal{M}_{u,E,M}$, and $\mathcal{M}_{t(P)}$ for the proton target and $\mathcal{M}_{s,M}$, $\mathcal{M}_{u,E,M}$, $\mathcal{M}_{t(P)}$, $\mathcal{M}_{t(V)}$, and $\mathcal{M}_c$ for the neutron one, where E and M stand for the terms including electric (proportional to e) and magnetic (proportional to $e\kappa_{N,\Theta}$) interactions. ϵ_γ and ϵ_{K^*} are the polarization vectors of the photon and the vector kaon, respectively. ϵ_Θ is the spin-1 component of the Rarita-Schwinger field for the Θ^+ [13]. We simplify the spin $3/2$ RS propagator by that of spin $1/2$ baryon. It was shown that this simplification worked qualitatively well in the low-energy regions [13]. The evaluation of the invariant amplitudes for the spin $1/2$ is also performed similarly to that of spin $3/2$.

In the present work, we also take into account scalar meson $\kappa(800, 0^+)$ exchange in addition to K and K^* exchange. The relevant effective Lagrangians are defined as follows:

$$\begin{aligned}
\mathcal{L}_{\gamma\kappa K^*} &= g_{\gamma\kappa K^*} F_{\mu\nu} F^{\mu\nu}_{K^*} \kappa, \\
\mathcal{L}_{\kappa N\Theta_3} &= \frac{g_{\kappa N\Theta_3}}{M_\kappa} \bar{\Theta}^\mu_3 (\partial_\mu \kappa) \Gamma_5 \gamma_5 N, \\
\mathcal{L}_{\kappa N\Theta_1} &= i g_{\kappa N\Theta_1} \bar{\Theta}_1 \Gamma_5 \kappa N,
\end{aligned} \tag{14}$$

where κ indicates the scalar meson field with its physical mass $\sim$800 MeV [28]. Because there is no information of the coupling constants $g_{\gamma\kappa K^*}$ and $g_{\kappa N\Theta_3}$, we estimate them for both the spin $3/2$ and $1/2$ Θ^+ as follow as a trial:

$$g_{\gamma\kappa K^*} = |g_{\gamma K K^*}| \text{ and } g_{\kappa N\Theta_3} = |g_{K N\Theta_3}|.$$

We note that the signs of these coupling constants are unknown and not estimated by flavor SU(3) symmetry. However, we verified that the signs of these coupling constants do not make significant differences in the numerical results. Hence, we consider only plus signs for the coupling constants. The reaction amplitudes for κ exchange [$t(S)$] can be written as follows:

$$\begin{aligned}
i\mathcal{M}_{3,t(S)} = &-\frac{2 g_{\gamma\kappa K^*} g_{\kappa N\Theta_3}}{M_\kappa} \frac{\bar{u}(p_2)\Gamma_5\gamma_5 u(p_1)}{q_t^2 - M_\kappa^2} [\epsilon_\Theta \cdot q_t] \\
&\times [(k_1 \cdot k_2)(\epsilon_\gamma \cdot \epsilon_{K^*}) - (\epsilon_\gamma \cdot k_2)(k_1 \cdot \epsilon_{K^*})] F_{t(S)}, \\
i\mathcal{M}_{1,t(S)} = &-2i g_{\gamma\kappa K^*} g_{\kappa N\Theta_1} \frac{\bar{u}(p_2)\Gamma_5 u(p_1)}{q_t^2 - M_\kappa^2} [(k_1 \cdot k_2)(\epsilon_\gamma \cdot \epsilon_{K^*}) \\
&- (\epsilon_\gamma \cdot k_2)(K_1 \cdot \epsilon_{K^*})] F_{t(S)}.
\end{aligned} \tag{15}$$

As shown in Eqs. (12), (13), and (15), we employ the four-dimensional form factors [13] defined as follows:

$$\begin{aligned}
F_x(q^2) &= \frac{\Lambda^4}{\Lambda^4 + \left(x - M_x^2\right)^2}, \quad x = s, t(P/V/S), u, \\
F_c &= F_u + F_{t(V)} - F_u F_{t(V)} \text{ for neutron}, \\
F_c &= F_s + F_u - F_s F_u \text{ for proton},
\end{aligned} \tag{16}$$

where M_x is the mass of the interchanged particle in the x channels. We verified that the inclusion of the form factor maintains the gauge invariance. We make use of the cutoff value $\Lambda = 750$ MeV as in Refs. [12,13].

III. NUMERICAL RESULTS

We present in this section the numerical results of the total and differential cross sections, asymmetries, and momentum-transfer t dependences for the neutron and proton targets. Here, the asymmetry is defined as follows:

$$\text{Asymmetry} = \frac{(d\sigma/d\Omega)_\perp - (d\sigma/d\Omega)_\parallel}{(d\sigma/d\Omega)_\perp + (d\sigma/d\Omega)_\parallel}. \tag{17}$$

The notations $\parallel$ and $\perp$ in Eq. (17) stand for the photon polarizations that are parallel and perpendicular to the reaction plane, respectively.

In Fig. 2, we show various contributions to the total cross sections for each kinematical channel separately as functions of photon energy in the laboratory frame (E_γ^{lab}). The upper two panels represent the results for the $\Theta^+(3/2^+)$, where we see that the contact and psuedoscalar K-exchange terms are main contributions for the neutron target, whereas the K-exchange term dominates the reaction for the proton one. Because the $\gamma K^* K$ coupling constants for the proton and neutron targets differ by $g_{\gamma K^0 \bar{K}^{*0}}/g_{\gamma K^+ K^{*-}} \sim 1.5$, we obtain the contribution of K exchange to the total cross sections for the proton target about two times larger than the neutron one. Being different from $\Theta^+(3/2^+)$, κ and K exchanges govern the reaction for the $\Theta^+(3/2^-)$ as demonstrated in the lower two panels. The total cross sections of K exchange for $\Theta^+(3/2^-)$ becomes much larger than those of $\Theta^+(3/2^+)$ due to the d-wave coupling for the $KN\Theta_3$ vertex. The large contribution of κ exchange can be understood by that we assumed larger coupling constants $g_{\kappa N\Theta}$ and $g_{\kappa\gamma K^*}$ for $\Theta^+(3/2^-)$ than those of $\Theta^+(3/2^+)$. However, even if we ignore κ exchange, the qualitative tendency $\sigma_{3/2^+} < \sigma_{3/2^-}$ is not altered, because K exchange is more dominant than the contributions from the κ exchange. Moreover, though we can see a difference of about two or three times in magnitudes of the total cross sections between the neutron and proton targets, the difference is much smaller than that of the Λ^* photoproduction associated with the pseudoscalar kaon as shown in the previous work [12].

In Fig. 3 we show the total (upper left) and differential (upper right) cross sections, the asymmetry (lower left) due to the different photon polarizations and the momentum transfer t dependence (lower-right) for $\Theta^+(3/2^+)$. The total cross sections from the neutron (solid line) and proton (dashed line) targets differ by little; the proton case is slightly larger due to the ratio $g_{\gamma K^0 \bar{K}^{*0}}/g_{\gamma K^+ K^{*-}} \sim 1.5$. The differential cross sections are calculated at two different photon energies, i.e., $E_\gamma^{\text{lab}} = 3.0$ GeV (thin curves) and 3.5 GeV (thick curves). The angle θ denotes the one between the incident photon and outgoing K^* in the center-of-mass frame. It is clearly shown that the differential cross section in the forward direction is strongly enhanced; it is mainly due to K exchange. We also find that κ exchange increases the differential cross section in the forward direction. The asymmetry behaves similarly in general for the proton and neutron targets as shown in the lower-left panel of Fig. 3. The sign of the asymmetry is negative when K exchange dominates the process. The momentum transfer t dependences are drawn in the lower-right panel. The t dependences show again the strong enhancement

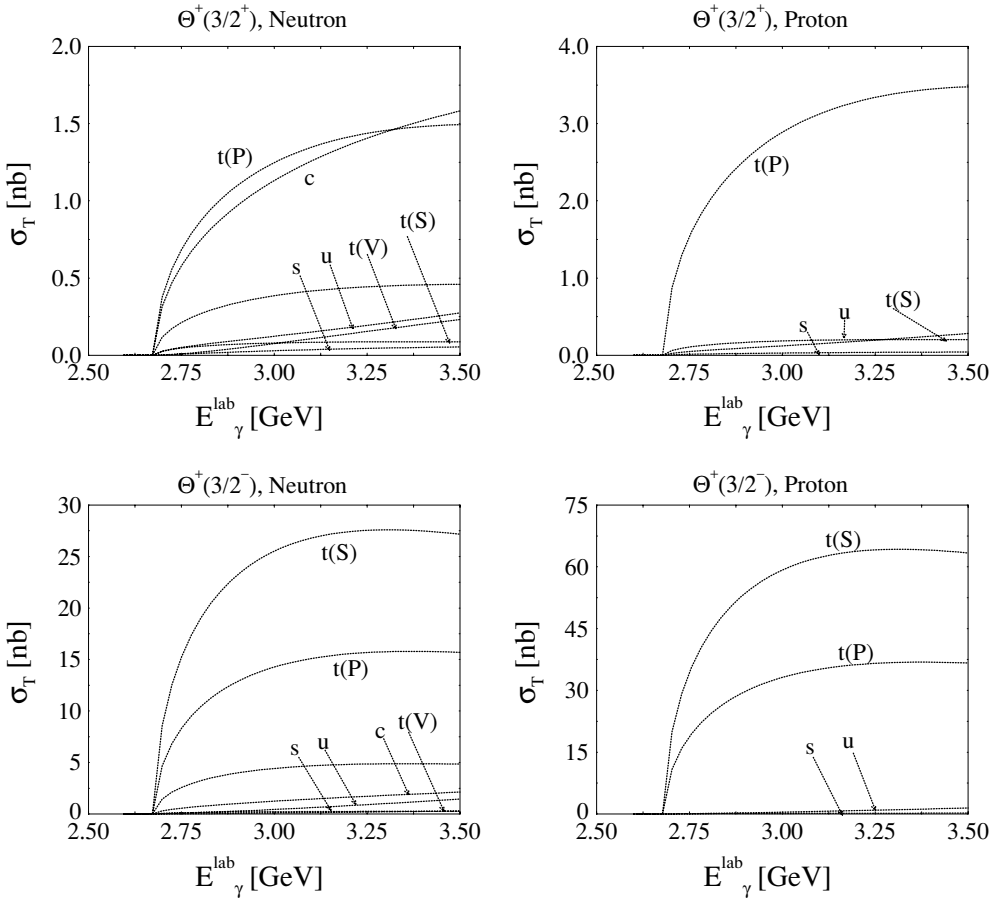

FIG. 2. Various contributions to the total cross sections from different kinematical channels. The labels are defined by s (s channel), u (u channel), t (P) (pseudoscalar kaon exchange in t channel), t (V) (vector kaon exchange in t channel), t (S) (scalar κ exchange in t channel) and c (contact term). We show the four different cases, i.e., $\Theta^+(3/2^+)$ from the neutron (upper left) and proton (upper right) targets, and $\Theta^+(3/2^-)$ from the neutron (lower left) and proton (lower right) ones.

in forward scattering. Also, we verified that the dependence on the coupling constants $g_{\gamma\kappa K^*}$ and $g_{\kappa N\Theta_3}$ is not significant, because the contribution of κ [$t(S)$] is small as shown in the upper-left panel of Fig. 2. Even for the case that we use $g_{\gamma\kappa K^*} = 2|g_{\gamma K K^*}|$ and $g_{\kappa N\Theta_3} = 2|g_{K N\Theta_3}|$, only 25% or less difference appears in the order of magnitudes of the total cross sections. Furthermore, other observables are not changed much by this choice.

Now, we turn to the results for the $\Theta^+(3/2^-)$ depicted in Fig. 4. The total cross sections turn out to be about a few 10s of times larger than those for the $\Theta^+(3/2^+)$. The angular distributions (differential cross sections and the momentum transfer t dependence) are rather similar to those for $\Theta^+(3/2^+)$, because the contributions of K and κ exchanges enhance the forward scattering. However, the asymmetries are distinguished clearly from the case of the $\Theta^+(3/2^+)$. The asymmetries for the $\Theta^+(3/2^-)$ production are in general positive when κ exchange dominates. However, if κ exchange is switched off, the asymmetries becomes similar to those for the $\Theta^+(3/2^+)$ production with negative sign due to K exchange dominance, which indicates that κ exchange plays a key role in distinguishing $\Theta^+(3/2^-)$ from the positive-parity one.

We note that, however, the dependence on the couplings of scalar κ in the case of the negative-parity is not ignored, being different from the previous case of positive-parity. This aspect can be easily verified by the curves shown in the lower-left panel of Fig. 2 in which the κ exchange in the t channel, $t(S)$, is the dominant contribution. Thus, the choice of $g_{\gamma\kappa K^*} = 2|g_{\gamma K K^*}|$ and $g_{\kappa N\Theta_3} = 2|g_{K N\Theta_3}|$ enhances the magnitudes of the total cross sections by a factor more than $\sim$10. For instance, we obtain $\sim$420 nb at $E_\gamma = 3.0$ GeV for the $\Theta^+(3/2^-)$ photoprodution from the neutron target. Despite the strong dependence on these coupling constants, the angular distributions are not much affected and show the strong forward enhancement. The asymmetry defined in Eq. (17) becomes all positive for the neutron and proton targets with a similar shape as shown in the lower-left panel of Fig. 3.

From here, we compare the results of spin 1/2 Θ^+ with the spin 3/2 Θ^+ photoproduction in Fig. 5. Here, we consider only the case of the positive-parity Θ^+, because the cross sections for the negative-parity one are in general about 10 times smaller than those for the positive-parity Θ^+ (see, for example, Ref. [24]). However, we note that the contribution of κ exchange was not considered in the former studies [24]. The

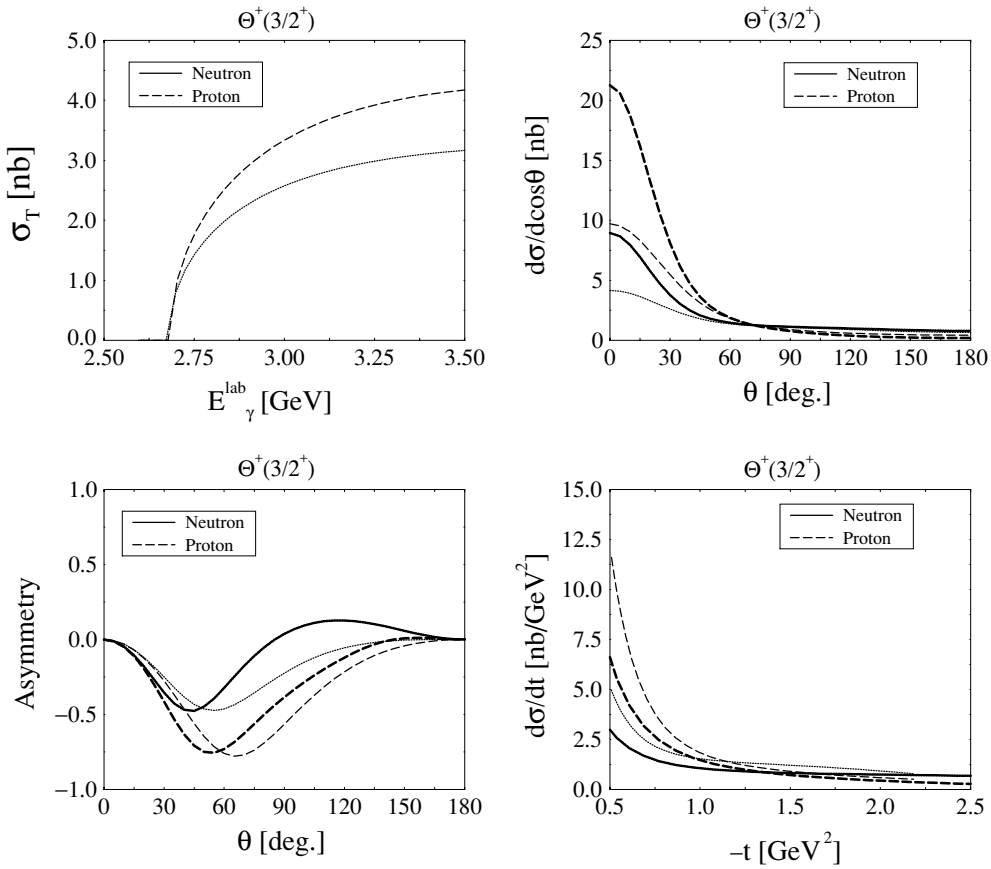

FIG. 3. The total (upper left) and differential (upper right) cross sections, the asymmetry (lower right), and the momentum-transfer t dependence (lower right) for $\Theta^+(3/2^+)$. The solid and dashed curves represent the results from the neutron and proton targets, respectively. Thin curves denote those calculated at $E_\gamma^{\rm lab} = 3.0$ GeV, whereas thick ones stand for those at $E_\gamma^{\rm lab} = 3.5$ GeV.

total cross sections are of a few nanobarns similarly to and slightly larger than that of $\Theta^+(3/2^+)$. We also observe that the angular distribution is enhanced strongly in the forward direction. The sign of the asymmetry depends on the type of the target; for the proton target it is positive, whereas for the neutron one negative. We have checked that the contribution from the tensor terms proportional to $g^T_{K^*N\Theta_1}$ makes the cross sections larger only by $\sim$10% [see Eq. (9)] when $g^T_{K^*N\Theta_1} = |g^V_{K^*N\Theta_1}|$. It also turns out that the effects from the tensor terms on the angular distribution and asymmetry are negligible. However, again, rather strong dependence on the coupling constants of $g_{\gamma\kappa K^*}$ and $g_{\kappa N\Theta_3}$ are observed as shown in the case of $\Theta^+(3/2^-)$. Especially, the asymmetry becomes all positive having peaks at $\sim 70^\circ$ for the neutron and proton.

IV. REACTION ANALYSIS VIA THE PHOTON AND K^* POLARIZATIONS

Last but not least, we discuss the analysis of the polarizations of the photon and the vector K^* meson. because the K^* meson can decay into the pseudoscalar kaon and pion, it is possible to determine the polarization state of K^* by the measured azimuthal distribution of the kaon and pion. By doing this, we can tell what meson exchange in the present reaction plays a dominant role. Similar analysis can be extended to other spin 3/2 as well as spin 1/2 baryon productions.

For this purpose, we first fix the photon polarization to be perpendicular to the reaction plane. Then, as clearly shown in Eq. (13), the K^* exchange contribution disappears, because it is proportional to $k_2 \cdot \epsilon_\gamma$, in which k_2 and ϵ_γ denote the outgoing K^* momentum and photon polarization vector, respectively. Now, let us set the polarization vector of K^*, ϵ_{K^*}, to be parallel to the direction of ϵ_γ. In this case, examining the $\epsilon_{\mu\nu\sigma\rho}$ structure of K exchange in Eq. (13), one can easily see that the contribution of K exchange vanishes. Thus, as shown in the panels on left side of Fig. 6, only κ exchange survives for both the positive (in the upper panel of Fig. 6) and negative (in the lower panel of Fig. 6 parity Θ^+). We also observe that κ exchange dominates the reaction even when we include all channels, as depicted by the curve labeled Total in Fig. 6. However, we note that the strengths of the κ exchange contribution depends on the unknown $\kappa N\Theta$ and $\gamma\kappa K^*$ coupling constants.

We now proceed to examine the case when the two polarization vectors are perpendicular to each other. As in the parallel case, the photon polarization vector is fixed to be perpendicular to the reaction plane so that K^* exchange can be eliminated. The corresponding results are shown

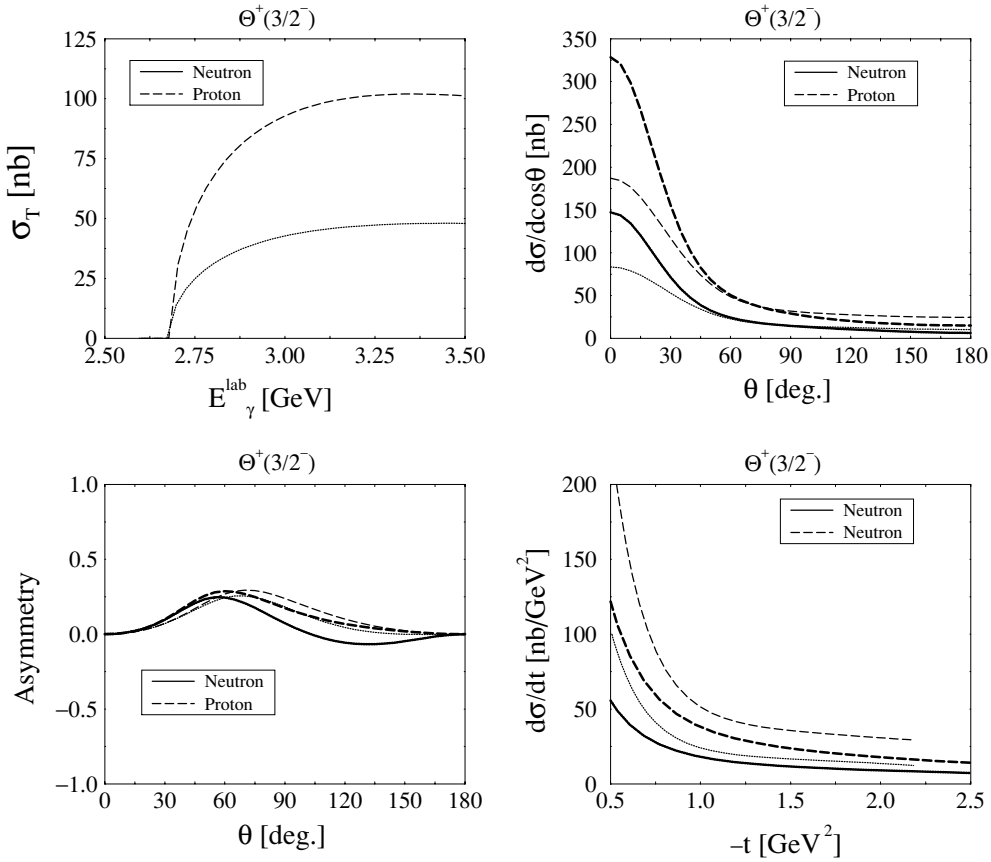

FIG. 4. The total (upper left) and differential (upper right) cross sections, the asymmetry (lower right), and the momentum-transfer t dependence (lower right) for $\Theta^+(3/2^-)$. The solid and dashed curves represent the results from the neutron and proton targets, respectively. Thin curves denote those calculated at $E_\gamma^{\rm lab} = 3.0$ GeV, whereas thick ones stand for those at $E_\gamma^{\rm lab} = 3.5$ GeV.

in the right side of Fig. 6. The amplitude of κ exchange turns out to be zero, because the term in the bracket of Eq. (15) vanishes. Therefore, the contribution comes only from pseudoscalar K exchange. Experimentally, the comparison of the two polarization combinations, $\epsilon_\gamma \perp \epsilon_{K^*}$ and $\epsilon_\gamma \parallel \epsilon_{K^*}$, provide information of the strengths of the $KN\Theta$ and $\kappa N\Theta$ coupling constants.

The bump or the increase in the differential cross sections for $\theta \gtrsim 60^\circ$ as shown in the right side of Fig. 6 is mainly due to the contact term contribution. The total contributions do not differ much from the cases with the K-exchange contribution only. Interestingly, the results for the two different parities of Θ^+ are rather similar each other except for the order of magnitudes, because the polarization dependence arises only from the structure of the $\gamma K^* M(K, K^*, \kappa)$ coupling, but not from that of $MN\Theta^+$, which carries the information of the parity of Θ^+.

The polarization analysis of the photon and vector K^* sheds light on determining which meson exchange is dominant in the present reaction. Though we do not show the results for the $\Theta^+(1/2^+)$-photoproduction explicitly here, we verified that the similar conclusion was drawn. We notice that this analysis may also be of great use in determining which meson is the most prominent in general $\gamma N \to M(1^-)B$ reactions, because the method discussed here is based only on the structure of the photon-meson-meson vertices, but not of vertices including baryons.

V. SUMMARY AND CONCLUSION

We have investigated the photoproduction of the exotic pentaquark baryon Θ^+ via the reaction process $\gamma N \to \bar{K}^*\Theta^+$, assuming that Θ^+ has spin 3/2. The effective Lagrangian approach was employed with phenomenological form factors [12,13]. We used the coupling constant for the $K^*N\Theta(3/2)$ vertex estimated from the constituent quark model. We also considered scalar meson $\kappa(800, 0^+)$ exchange. We assumed the following relations for the coupling constants; $g_{\gamma\kappa K^*} = g_{\gamma K K^*}$ and $g_{\kappa N\Theta} = g_{KN\Theta}$ as a trial. The main results of the present work are summarized in Table II.

In the present work, we did not find large difference between the total cross sections from the neutron and proton targets, which is different from the conclusion of the previous work of $\gamma N \to \bar{K}\Theta^+(3/2)$ [12]. The reason lies in the fact that the contact term in the present case does not provide a large contribution to the cross sections, compared

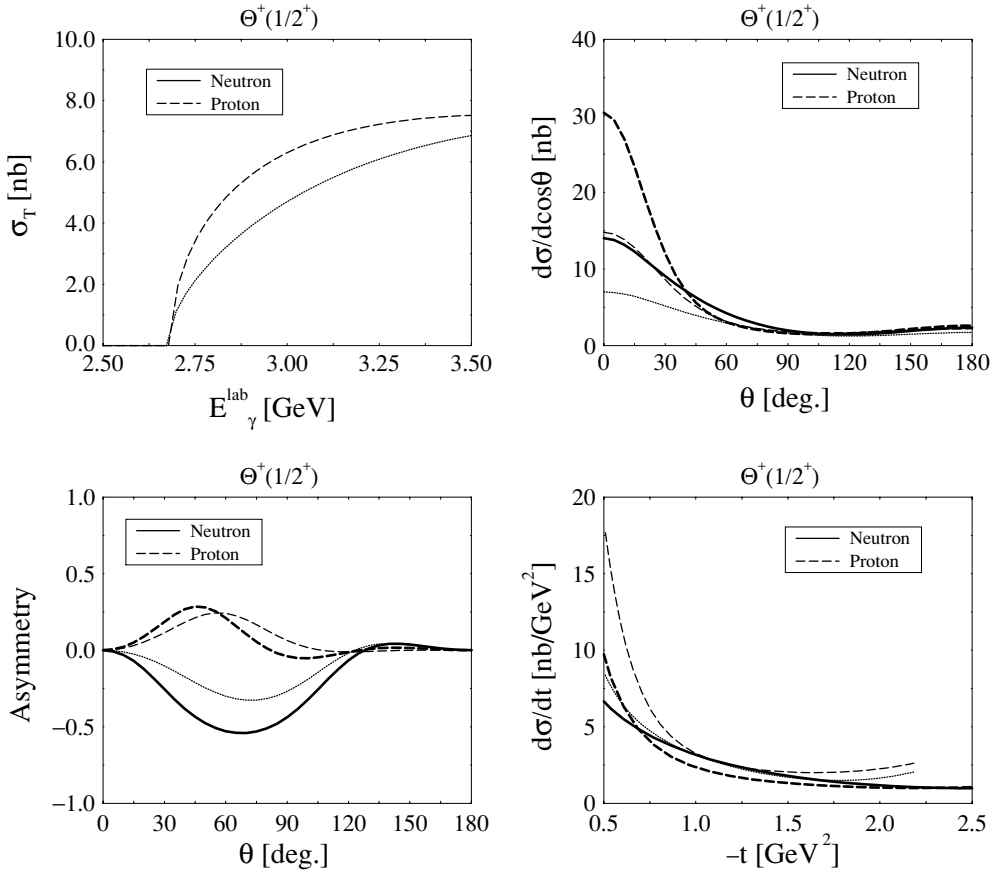

FIG. 5. The total (upper left) and differential (upper right) cross sections, the asymmetry (lower right), and the momentum-transfer t dependence (lower right) for $\Theta^+(1/2^+)$. The solid and dashed lines represent the results from the neutron and proton targets, respectively. Thin lines are for the results calculated at $E_\gamma^{\rm lab} = 3.0$ GeV, whereas thick lines for done at $E_\gamma^{\rm lab} = 3.5$ GeV.

to other meson exchange. These differences between the Θ^+ photoproductions with the pseudoscalar K and with the vector K^* can be useful to determine the spin quantum number of the Θ^+ baryon. We estimated the total cross sections for the present reaction qualitatively as follows: $\sigma_{3/2^+} \sim 1.5$ nb and $\sigma_{3/2^-} \sim 50$ nb for the energy regions of $E_{\rm th} \lesssim E_\gamma^{\rm lab} \lesssim 3.5$ GeV for both the neutron and proton targets. We notice that there is the model dependence due to the coupling constants of κ exchange, in particular, in the case of $\Theta^+(3/2^-)$. However, the tendency $\sigma_{\Theta^+(3/2^+)} < \sigma_{\Theta^+(3/2^-)}$ is rather stable, because psuedoscalar K exchange, which has less dependence on the model parameters, is the most dominant contribution in the present reaction.

In angular distributions, we observed a large enhancement in the forward region due to the t-channel dominance (K and κ exchanges) for both the spin $1/2$ and spin $3/2$ cases. From these observations, we expect that in the laboratory frame, there must be even stronger forward enhancement for the outgoing K^*. The asymmetry shows relatively clear difference between the positive and negative parities of the $\Theta^+(3/2)$, though there is one caveat: once we know the strengths of the coupling constants $g_{\gamma\kappa K^*}$ and $g_{\kappa N\Theta}$. We also compared the present results to those from the reaction with the $\Theta^+(1/2^+)$.

Finally, an analysis was proposed to determine which meson exchange is dominant in the t-channel, with the photon and K^* polarizations being explicitly considered. It was observed that scalar meson κ exchange only survives when the polarizations of the photon and K^* are parallel. On the contrary, when these polarizations are perpendicular to each

TABLE II. Main results of the Θ^+-photoproduction via $\gamma N \to \bar{K}^* \Theta^+$.

J^P	$3/2^+$		$3/2^-$		$1/2^+$	
Target	n	p	n	p	n	p
σ at $E_\gamma^{\rm lab} = 3.0$ GeV	∼2.5 nb	∼3.2nb	∼40 nb	∼90 nb	∼4 nb	∼5.5 nb

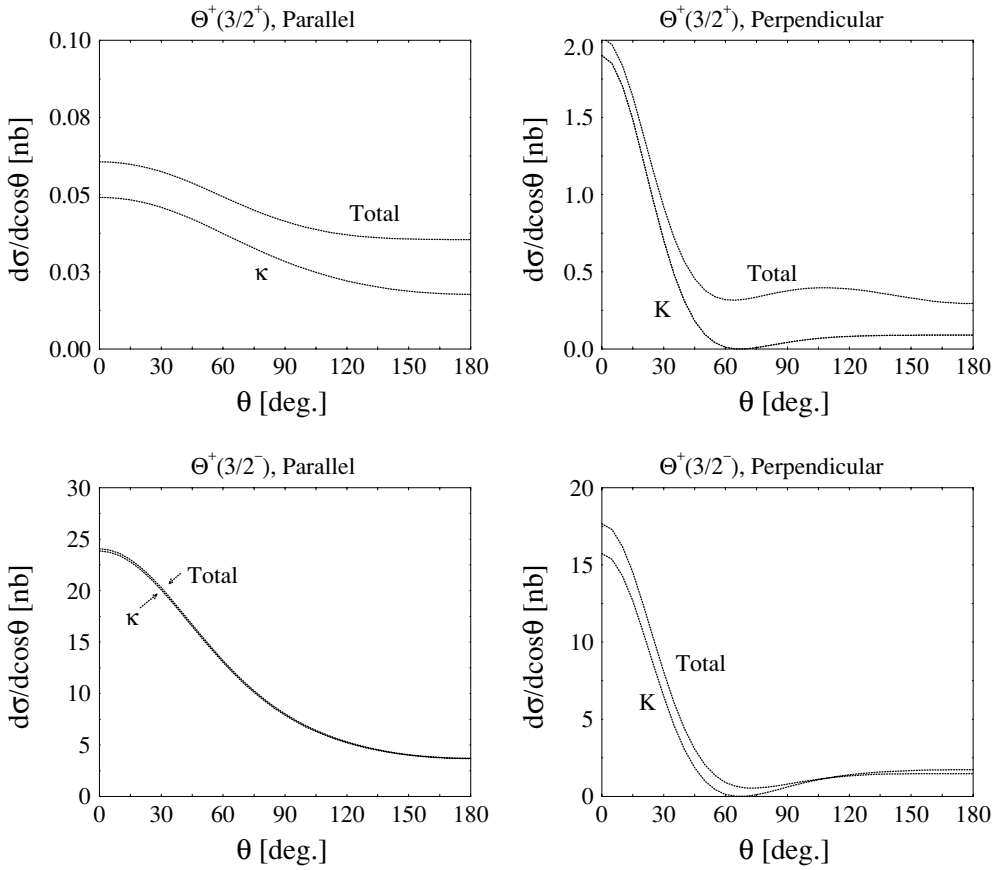

FIG. 6. Differential cross sections when the photon and K^* are polarized in parallel (left) and perpendicular (right) to each other. We consider the states of $J^P = 3/2^+$ (upper panels) and $3/2^-$ (lower panels).

other, pseudoscalar K exchange turns out to be dominant. This analysis may be applied to a general reaction $\gamma N \to M(1^-)B$.

We note that the coupling constants $g_{\gamma\kappa K^*}$ and $g_{\kappa N\Theta}$, being important in the present investigation, are not known well. Especially, the asymmetry is affected much by the different choices of the coupling constants for the cases of $\Theta^+(3/2^-)$ and $\Theta^+(1/2^+)$, whereas the cross sections are changed only in the order of the magnitudes. Considering the rather small values shown in Table II, it might be rather difficult to observe a clear peak from the present reaction process in the present experimental facilities. However, because we once again observed strong forward scattering enhancement that could be measured most appropriately by LEPS, it is expected that different experimental setup may obtain sizable statistics for the indication of Θ^+ for the present reaction process.

ACKNOWLEDGMENTS

We are very grateful to J. K. Ahn, V. Koubarovski, T. Nakano, and T. Hyodo for fruitful discussions. The work of S.I.N. has been supported in part by the scholarship from the Ministry of Education, Culture, Science and Technology of Japan. A. H. was supported in part by the Grant for Scientific Research [(C) no. 16540252] from the Education, Culture, Science and Technology of Japan. H.C.K. and S.I.N. were supported by a Korea Research Foundation grant funded by the Korean government (MOEHRD) (KRF-2005-202-C00102).

[1] D. Diakonov, V. Petrov, and M. V. Polyakov, Z. Phys. A **359**, 305 (1997).
[2] T. Nakano *et al.* (LEPS Collaboration), Phys. Rev. Lett. **91**, 012002 (2003).
[3] K. H. Hicks, Prog. Part. Nucl. Phys. **55**, 647 (2005).
[4] R. A. Schumacher, nucl-ex/0512042.
[5] K. H. Hicks (CLAS Collaboration), hep-ex/0510067.
[6] M. Battaglieri *et al.* (CLAS Collaboration), Phys. Rev. Lett. **96**, 042001 (2006).
[7] B. McKinnon *et al.* (CLAS Collaboration), Phys. Rev. Lett. **96**, 212001 (2006).
[8] S. Niccolai (Clas Collaboration), hep-ex/0604047.
[9] T. Nakano, for instance, talk given at the workshop Pentaquark05, J-Lab, 20–22 October, 2005.

[10] V. V. Barmin *et al*. (DIANA Collaboration), hep-ex/0603017.
[11] K. Miwa *et al*. (KEK-PS E522 Collaboration), Phys. Lett. **B635**, 72 (2006).
[12] S. i. Nam, A. Hosaka, and H.-Ch. Kim, Phys. Lett. **B633**, 483 (2006).
[13] S. i. Nam, A. Hosaka, and H.-Ch. Kim, Phys. Rev. D **71**, 114012 (2005).
[14] D. P. Roy, J. Phys. G **30**, R113 (2004).
[15] W. Liu and C. M. Ko, Phys. Rev. C **68**, 045203 (2003).
[16] W. Liu and C. M. Ko, Nucl. Phys. **A741**, 215 (2004).
[17] Y. S. Oh, H. C. Kim, and S. H. Lee, Phys. Rev. D **69**, 014009 (2004).
[18] S. Janssen, J. Ryckebusch, D. Debruyne, and T. Van Cauteren, Phys. Rev. C **65**, 015201 (2002).
[19] R. B. Clark, Phys. Rev. D **1**, 2152 (1970).
[20] M. Clark and A. Donnachie, Nucl. Phys. **B125**, 493 (1977).
[21] B. J. Read, Nucl. Phys. **B52**, 565 (1973).
[22] M. Gourdin, Nuovo Cimento **36**, 129 (1965); **A40**, 225 (1965).
[23] R. Machleidt, K. Holinde, and C. Elster, Phys. Rept. **149**, 1 (1987).
[24] S. i. Nam, A. Hosaka, and H.-Ch. Kim, Phys. Lett. **B579**, 43 (2004).
[25] K. S. Choi, S. i. Nam, A. Hosaka, and H.-Ch. Kim, Phys. Lett. **B636**, 253 (2006).
[26] H.-Ch. Kim, M. Polyakov, M. Praszalowicz, G. S. Yang, and K. Goeke, Phys. Rev. D **71**, 094023 (2005).
[27] Y. Azimov, V. Kuznetsov, M. V. Polyakov, and I. Strakovsky, Eur. Phys. J. A **25**, 325 (2005).
[28] S. Eidelman *et al*. [Particle Data Group], Phys. Lett. **B592**, 1 (2004).
[29] F. E. Close and J. J. Dudek, Phys. Lett. **B586**, 75 (2004).
[30] A. Hosaka, M. Oka, and T. Shinozaki, Phys. Rev. D **71**, 074021 (2005).